Advances in Intelligent Systems Research, volume 159
International Conference on Mathematics, Modelling, Simulation and Algorithms (MMSA 2018)

Research on Influence of Temperature Variation on Deformation of Inflatable Wing Skin Film

Longbin Liu, Zhengyu Jiang, Ke Peng*, Fan Hu and Huabo Yang
College of Aerospace Science and Engineering, National University of Defense Technology, Deya Road, Changsha, 410073, China
*Corresponding author

***Abstract*—With many advantages of foldable, small size, good portability, easy loading and transportation, rapid deployment, and easy launch, the flexible inflatable wing has attracted the attention of scholars and engineers abroad. However, the ambient temperature variation directly affects the internal pressure of the inflatable wing, which produces significant complex deformation of the wing skin film. In this paper, the influence of different temperature conditions on the pressure change of the flexible inflating wing is studied, and the ABAQUS finite element modeling method is used to simulate the wing skin film under different temperature conditions (25°C, 35°C, 45°C, 55°C). The result shows that strain deformation characteristics and data structure indicate that the strain change of the skin film is closely related to the ambient temperature, and the temperature changes will cause the internal and external pressure difference to increase, and the strain near the wing root and the wing tip will become larger, and the law of strain variation along the spanning characteristic line and the chord-wise characteristic line is discussed, which provides an effective reference for the analysis and design of the inflatable mechanical deformation of the flexible inflatable membrane structure (wing).**

Keywords—inflatable wing; strain characteristics; temperature change; flexible skin film; finite element simulation

I. INTRODUCTION

Folding flexible inflatable wing has gradually become a new type of structural bearing and weight reduction technology due to its unique advantages of light weight, portability, small folding volume, increased lift, drag reduction, ease of transportation, rapid deployment, low cost and so on. The application field is more and more extensive, which has more and more important research value and engineering application prospects [1-7]. The most typical was the NASA-I-2000 flexible aerated wing aircraft developed by NASA and conducted low-level flight test development, which technically verified the feasibility of the aerated wing to achieve flight [8-9]. Elam DB [10] designed a flexible inflatable wing composed of a flexible material with expandable structure, and while in the deflated and stored state, the occupied volume was small; compared with fully inflating and deploying, the wing had enough structural rigidity. Usui Michiko et al. [11] studied the feasibility of inflating deployment and flight tests at higher altitudes of an inflated winged UAV. Jamey D [12] carried out the structural design, modeling, ground testing and flight tests of UAV flexible inflating wings, and obtained a prediction of the torsional deformation of the inflated wing and the required inflation pressure. And the relationship between the stiffness of the inflatable wing and the internal pressure as well as the external load is also analyzed. However, these studies did not consider the effect of temperature changes on the deformation characteristics of the flexible inflatable wing. Therefore, it is necessary to comprehensively consider the structural weight of the wing skin film material, the inflation pressure, the ambient temperature, the aeration rate and other factors on the carrying capacity of the flexible wing film skin to study the effect of deformation characteristics, which could provide an effective reference for the analysis and design of the inflatable mechanics deformation of the flexible inflatable film wing.

II. SKIN FILM DEFORMATION ANALYSIS

A. Skin Film Strain Analysis

Inflatable wing skin film is generally a two-phase plane stress state under the action of internal and external pressure difference loads [6]. The physical relationship of the biaxial stress and the deformation of the skin membrane between the inflated internal and external pressure can be expressed as:

$$\left(p_2 - p_1 - \rho g\right) = \frac{\sigma_x t}{R_x} + \frac{\sigma_y t}{R_y} \tag{1}$$

For anisotropic flexible skin materials, the biaxial stress-strain relationship in the x and y direction satisfies Hooke's law (μ is the Poisson's ratio of the skin film material):

$$\varepsilon_x = \frac{\sigma_x}{E_x} - \mu\frac{\sigma_y}{E_y}, \quad \varepsilon_y = \frac{\sigma_y}{E_y} - \mu\frac{\sigma_x}{E_x} \tag{2}$$

In the equation, R_x, R_z are the biaxial curvature deformation radius respectively. General flexible inflatable skin membrane material is isotropic material or fiber reinforced laminated anisotropic composite material, which needs to further consider the different effects of modulus in the x and y direction, which is denoted as E_x and E_y. The deformation in all directions can be further obtained based on the uniformity pressure load and the coordinating relationship between the biaxial deformation.

B. Effect of Temperature Changes on the Inflatable Wing

While the flexible aerated wing is formed, due to the large

elastic modulus of the skin film, the small deformation assumption is considered under the effect of the pressure difference. Then it could be considered that the inflatable wing volume remains the same, and the amount of air charge is not considered. Only the effect of ambient temperature changes on the internal and external pressure differential load of the internal aeration is studied. The load-carrying mechanical characteristics and deformation law with temperature changes are studied, and the gas state equation can be obtained:

$$\Delta PV=(P_2-P_1)V=nRT=\frac{m}{M}RT \tag{3}$$

Here, ΔP indicates the pressure difference between the inside and outside of the flexible wing, V indicates the volume, R is the gas constant, T is the quasi-static gas temperature, M is the internal gas molar mass, and m is the internal gas actual mass, the method of the small deformation equal volume is used to calculate the equivalent inflation pressure at different temperatures. According to the above equations, the equivalent differential pressures under different temperature conditions (25°C (298.15K), 35°C (308.15K), 45°C (318.15K), 55°C (328.15K)) are calculated shown in Table 1.

TABLE I. INFLATABLE WING MODAL SIMULATION PARAMETERS

Tempera-ture /k	Air mass /g	Molecular mass	Gas constant	Volume /m^3	ΔP /Pa
298.15	0.000807224	29	8.31	0.002	1000
308.15	0.000807224	29	8.31	0.002	1033.54
318.15	0.000807224	29	8.31	0.002	1067.08
328.15	0.000807224	29	8.31	0.002	1100.62

According to the table data, the ABAQUS finite element simulation model can be set different internal and external pressure differential loads, and the corresponding strain deformation characteristics can be simulated and calculated.

C. Finite Element Modeling Simulation Analysis

The multi-air beam wing is used as the research object. The Vectran fiber-reinforced laminated composite film material is used for the inflatable wing film. The flexible wing under inflation is under aerodynamic loading, the upper and lower wing, and the internal air beam. But the internal gas pressure, the external pressure, and the aerodynamic load are all acting loads in the form of pressure and are set in the load of the simulation. The loads setting includes the upper wing pressure load, the lower wing pressure load, the side wing pressure load, and all the skin film's own gravity load. Due to the effect of aerodynamic loads on the upper and lower wings, the equivalent aerodynamic forces formed can be absorbed by a single wing. For ease observation, the equivalent aerodynamic load is set on the upper wing in the model as shown in Figure 1.

The wing mesh elements in the finite element simulation model all use matched Explicit membrane. For the upper and lower wing surface, the swept quadrilateral mesh is used to improve the stability and division accuracy,. And the cell type is M3D4R four-node quadrilateral membrane element, reduced integration, and hourglass control. The flanking surface adopts a free triangle mesh assigned mesh control attribute parameter, and the unit type is an M3D3 three-node triangular membrane element. The air beam puller adopts a triangular mesh assigned mesh to control the attribute parameters.

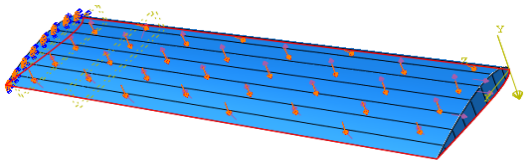

FIGURE I. LOADING PARAMETERS OF EACH FACE OF THE INFLATABLE WING

III. SIMULATION RESULTS AND DISCUSSION

A. Simulation Analysis of Strain Deformation at Different Temperatures

Based on the ABAQUS FEM model, by setting different internal and external pressure loads, the strain cloud diagrams obtained at different temperatures corresponding to 25°C, 35°C, 45°C, and 55°C, respectively, are shown in Figures 2-5.

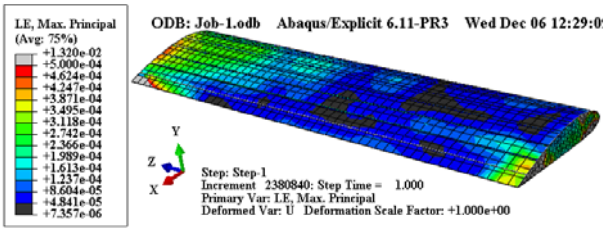

FIGURE II. STRAIN CLOUD AT 25°C

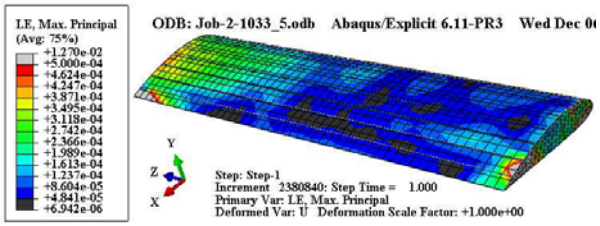

FIGURE III. STRAIN CLOUD AT 35°C

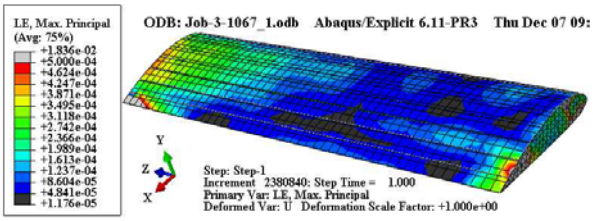

FIGURE IV. STRAIN CLOUD AT 45°C

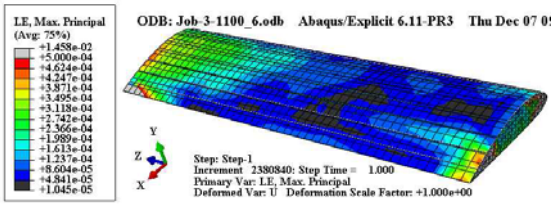

FIGURE V. STRAIN CLOUD AT 55°C

It can be seen that with rising of the temperature, the distribution of strain deformation is basically the same, and the values of the root wing and wing tip strain are significantly larger than that of the central area, and the temperature is higher, the gas pressure inside the inflatable is greater. As a result, the tensile stress and strain experienced by the skin film increase, and the equivalent strain and deformation area expands toward the central area of the wing. However, the strain value in the middle of the wing slightly decreases and changes continuously along the chord-wise direction. This is because the upper wing surface of the wing bears the aerodynamic load in the simulation, and the partial compressive strain and the internal and external pressure difference cancel each other, which results that the change of the area's tensile strain value is relatively slow compared to other areas. The trailing edge near the wing has a larger strain deformation and a smaller leading edge. Therefore, the trailing edge of the wing needs a structural reinforcement design to prevent the wing from being slightly deformed and distorted.

B. Spanning and Chord Wise Strain Deformation Analysis

Based on the simulation results, the characteristic lines are selected at the spanning and the chord directions shown in Fig. 6. The spanning characteristic line is the middle position of the wing, which is the seventh grid line from the trailing edge. The chord-wise characteristic line is also in the middle, which is a little 25th grid line away from the wing. Extracting the calculation data, two spanning adjacent nodes and chord-wise adjacent to a node are selected respectively.

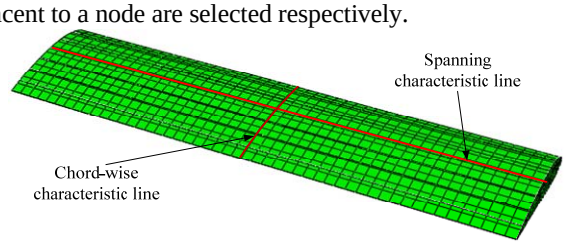

FIGURE VI. SPANNING AND CHORD-WISE FEATURE LINE

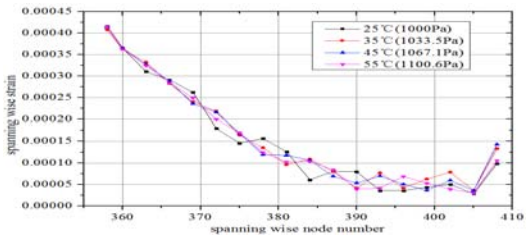

FIGURE VII. COMPARISON OF WING SPANNING AND CHORD-WISE CHARACTERISTIC STRAIN DATA

From the calculated strain cloud results, it can be seen that the strain changing trend in the spanning direction is basically the same as the temperature load increases, and the strain values gradually decrease from the wing root to the wing tip. However, due to the increasing of the temperature, the pressure inside the inflating wing increases, which results in the increasing of the pressure differential between the inside and outside of the wing, and the strain near the wing root and the wing tip slightly become larger, while the local spanning strain near the middle of the wing decreases. This is due to the increasing of the differential pressure between the inside and outside pressure and the warping deformation degree of the wing is weakened. Moreover, the spanning and chord-wise tensile stress of the wing upper wing skin and the compressive stress caused by the warpage partially cancel each other.

TABLE II. CHORD CHARACTERISTIC LINE STRAIN UNDER DIFFERENT TEMPERATURES

Serial NO.	Node NO.	25 ℃	35 ℃	45℃	55 ℃	35℃ Increeme	45℃ Increment	55℃ Increment
1	128	7.7173E-05	8.7292E-05	9.5171E-	0.00007398	1.01188E-05	1.79985E-05	-3.1936E-06
2	230	9.1340E-05	0.00013212	0.00139800	9.1003E-05	4.08418E-05	4.85578E-05	-3.365E-07
3	332	8.3294E-05	0.00011918	0.00136900	0.00010252	3.58236E-05	5.36686E-05	1.92336E-05
4	434	7.3126E-05	7.4327E-05	8.656E-05	9.9059E-05	1.2007E-06	1.34433E-05	2.59334E-05
5	536	0.00006881	4.8911E-05	5.431E-05	8.8623E-05	-1.98984E-05	-1.44912E-05	1.98134E-05
6	638	5.1022E-05	3.3835E-05	3.995E-05	6.4379E-05	-0.000017187	-1.10632E-05	1.33567E-05
7	740	0.00008291	0.00010547	0.00101111	7.9769E-05	0.00002255	0.00002818	-3.1469E-06

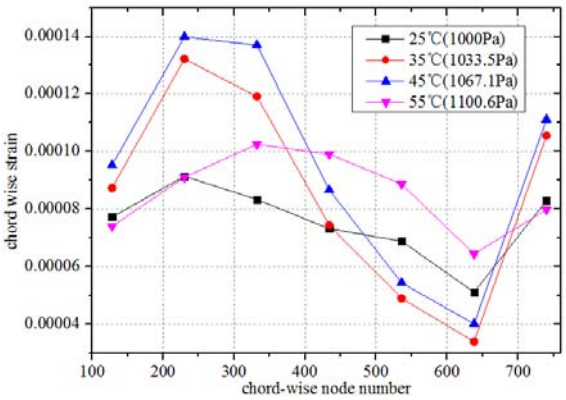

FIGURE VIII. COMPARISON OF STRAIN DATA OF WING CHORD-WISE CHARACTERISTIC LINE UNDER DIFFERENT TEMPERATURE LOADS

It can be seen from the chord-wise strain cloud results (shown in Table 2, Figure 8 and Figure9) that the strain trends in the chord-wise direction are exactly the same as the temperature load increases, but the strain changes and temperature gradients at the same node are the same, which is no positive correlation. It is also found that with the rising of the internal temperature of the flexible wing, the strain that appears at each node of the chord tends to be evenly changed, which results in the decreasing of the strain in the range of the larger strain near the leading edge of the wing, and the local

strain in the vicinity of the lower strain increases the strain changing law instead at the trailing edge of the wing.

TABLE III. SPANNING CHARACTERISTIC LINE STRAIN UNDER DIFFERENT TEMPERATURES

NO.	Node NO.	25℃	35℃	45℃	55℃	35℃ Increment	45℃ Increment	55℃ Increment
1	358	0.000415915	0.000407599	0.000414242	0.000414813	-8.316E-06	-0.0000016773	-0.0000001102
2	360	0.000364842	0.00036233	0.000364855	0.000362689	-2.512E-06	1.3E-08	-2.153E-06
3	363	0.000310590	0.00033244	0.000326881	0.000324104	0.00002185	0.00001629	0.00001351
4	366	0.000291028	0.00028284	0.000288031	0.000284431	-8.188E-06	-2.997E-06	-0.0000006597
5	369	0.000262277	0.000240053	0.00023584	0.000249332	-0.0000222224	-0.0000264	-0.0000129 45
6	372	0.000179799	0.000219044	0.000215866	0.00020001	0.00003924 5	0.00003606 7	0.00002021 1
7	375	0.000145458	0.000164327	0.000168353	0.000170006	0.00001886 9	0.00002289 5	0.00002454 8
8	378	0.000156674	0.000135399	0.000119299	0.000123797	-0.0000212 75	-0.0000373 75	-0.0000328 77
9	381	0.000125875	9.60562E-05	0.000117651	0.000101675	-2.98188E-05	-8.224E-06	-0.0000242
10	384	6.06698E-05	0.000108761	0.000105995	0.000103604	4.80912E-05	4.53252E-05	4.29342E-05
11	387	0.000080426	7.97028E-05	6.89736E-05	0.00008358	-7.232E-07	-1.14524E-05	3.154E-06
12	390	7.96488E-05	4.12588E-05	5.31837E-05	3.87757E-05	-0.0000383 9	-2.64651E-05	-4.08731E-05
13	393	3.56432E-05	7.69069E-05	6.95599E-05	4.16506E-05	4.12637E-05	3.39167E-05	6.0074E-06
14	396	3.57719E-05	4.20761E-05	5.04755E-05	6.83081E-05	6.3042E-06	1.47036E-05	3.25362E-05
15	399	4.32974E-05	0.00006242	3.61415E-05	5.29018E-05	1.91226E-05	-7.1559E-06	9.6044E-06
16	402	5.01859E-05	7.85357E-05	5.93565E-05	3.88492E-05	2.83498E-05	9.1706E-06	-1.13367E-05
17	405	2.82541E-05	3.61592E-05	3.54348E-05	0.00003025 7	7.9051E-06	7.1807E-06	2.0029E-06
18	408	9.86548E-05	0.000133147	0.000143006	0.00010564	3.44922E-05	4.43512E-05	6.9852E-06

IV. CONCLUSION

(1) With the increasing of the temperature, the gas pressure inside the aeration increasing causes the tensile stress and strain of the skin film to increase, and the equivalent strain deformation area expands to the central area of the wing. The deformation of the trailing edge near the wing is slightly larger, which needs a structural reinforcement design to prevent the wing from slightly deforming and twisting.

(2) With the increasing of temperature loadS, the strain changing trend in the spanning direction is basically the same, and gradually decreases from the wing root to the wing tip. However, the strain near the wing root and the wing tip slightly became larger, but the spanning strain near the middle areas decreases conversely.

(3) The strain changing trend in the chord-wise direction is exactly the same, but there is no positive correlation between the strain changing at the same location and the temperature gradient, which shows that the strain in each direction of the chord-wise tends to the uniform change.

ACKNOWLEDGMENT

The research was sponsored by the Research project of National University of Defense Technology (No. ZK16-03-33) and Hunan Natural Science Foundation (No. 2018JJ3591).

REFERENCES

[1] T. Yao, Y. Zhang, “Analysis of inflatable system for expandable spacecraft,” Internal Space. Beijing, vol. 1, pp. 32–35, 2008. (in chinese)

[2] H S Lafayette, “Computational investigation of flow over in floatable wings at maniple Reynolds numbers,” AIAA-2011-377, 2011.

[3] Q Zhang, Z Ye, “Novel Method Based on Inflatable Bump for Vertical Tail Buffeting Suppression,” Journal of Aircraft, vol. 52: pp. 367-371, 2015.

[4] J Li, H Wang, Y Fang, “Application of Flexible Inflatable Wings on Cruise Missiles,” Flying missile, vol. 8: pp. 60-64, 2015. (in chinese)

[5] Z Wang, H Wang, Q Jia, “Deflection prediction for inflatable wing based on artificial neural network,” Journal of Beijing University of Aeronautics and Astronautics, vol. 37: pp. 405-408, 2011.

[6] Y. Jia, Structural design and mechanical simulation of flexible inflatable wing, CHN: Graduation Thesis, 2017.

[7] L Liu, M Lv, H Xiao, et al, “Calculation and Simulation of Stratospheric Crew Cabin Stress Based on Gradient Pressure Gradient,” Beijing University of Aeronautics and Astronautics, vol. 40: pp. 1386-1391, 2014.

[8] B Glen, H Roy, “inflatable structures for Deployable wings,” AIAA, 2001-2068, 2001.

[9] E James, W Joseph, V Stephen, et al, “ground and flight evaluation of a small scale inflatable wing aircraft,” AIAA, 2002-0820, 2002.

[10] J Breuer, W Ockels, R Luchsinger, “An inflatable wing using the principle of Tensairity,” Proceedings 48th AIAA Structures, pp 1-12, 2007 [Structural Dynamics and Materials Conference, 2007].

[11] D Elam, “Inflatable aerodynamic wing and method,” U.S. Patent 7, 2007.

[12] A Simpson, A Santhanakrishnan, J Jacob, et al, “Flying on air: UAV flight testing with inflatable wing technology,” AIAA 3rd" Unmanned Unlimited" Technical Conference, Workshop and Exhibit, 2004.